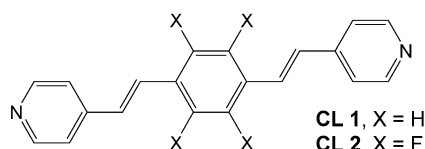


# Setting the Environmental Conditions for Controlling Gold Nanoparticle Assemblies\*\*

Meital Orbach, Michal Lahav, Petr Milko, Sharon G. Wolf, and Milko E. van der Boom\*

Nanoparticles (NPs) may be exploited to make practical materials that are capable of the selective detection of (bio)molecules.<sup>[1–7]</sup> Sensing with NPs often depends on the ability to selectively form aggregates. For instance, Mirkin et al. introduced a bio-barcode amplification method for ultrasensitive protein detection.<sup>[8]</sup> Another important study involves the detection of copper ions by hybrid AuNP assemblies in click chemistry.<sup>[9,10]</sup> The structures of AuNP-based assemblies can also be controlled electrochemically or by light.<sup>[11–13]</sup> However, despite these successes, controlling the properties and structure of NP-based assemblies with organic cross-linkers (CLs) still remains a challenge.<sup>[14]</sup> We have previously shown that the molecular geometry of CLs and the number of possible NP binding sites are related to the formation of hybrid AuNP assemblies and their associated optical properties.<sup>[15]</sup>

Herein we show that the aggregation and the optical properties of AuNP assemblies are related to the electronic properties of the CLs and the organic capping layers of the AuNPs. The molecular structures of the CLs are shown in Scheme 1 and consist of two vinylpyridine units bridged by an arene (**1**) or a fluorinated arene (**2**).<sup>[15–18]</sup> In this study, we



**Scheme 1.** Molecular structures of the cross-linkers (CLs)<sup>[15–18]</sup> used to generate assemblies with citrate- and TOAB-capped AuNPs.

compare the formation of AuNP assemblies in water and toluene using citrate- and tetraoctylammonium bromide (TOAB)-capped AuNPs, respectively.<sup>[19–22]</sup> Solutions of the CLs (50  $\mu$ M in THF) were added stepwise to citrate-capped AuNPs in water or to TOAB-capped AuNPs in toluene. A distinct color change from red to deep blue/purple was observed in all cases, indicating the formation of AuNP assemblies (Figure 1; Supporting Information, Figure S1, insets).<sup>[10,15]</sup> The UV/Vis spectra of the AuNP-based assemblies formed in water with citrate-capped AuNPs and CLs **1** and **2** show significant but different changes upon increasing the CL concentration from 0.0 to 3.7  $\mu$ M.

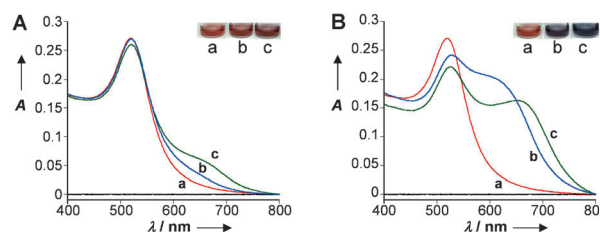


**Figure 1.** A, B) UV/Vis spectra in water of a) citrate-capped AuNPs and of the hybrid AuNP assemblies generated from mixing the AuNPs with THF solutions of b) CL **2** or c) CL **1** at two different final concentrations of the CL: A) [CL] = 1.0  $\mu$ M, B) [CL] = 2.8  $\mu$ M. Insets: photographs of solutions: (a), (b), and (c). The spectra were recorded 2 min after mixing the components and fivefold dilution.<sup>[23]</sup>

The intensity of the surface-coupled plasmon band at  $\lambda_{\text{max}} = 635\text{--}680$  nm increases with a concurrent intensity decrease of the band at  $\lambda_{\text{max}} \approx 519$  nm, which corresponds to unbound AuNPs (Supporting Information, Figure S1). The AuNP aggregation is more pronounced with CL **1** (Figure 1). Mechanistically, replacement of the negatively charged citrate-capping layer of the AuNPs by the CLs might be more favorable with an electron-rich system. The electron-poor fluorinated arene of CL **2** is likely to decrease the reactivity of its vinylpyridine units. Indeed, 2D  $^{15}\text{N}\text{--}^1\text{H}$  correlation NMR spectroscopy showed the nitrogen signal of CL **2** at  $\delta$  319.9 ppm, which is 4.2 ppm downfield than that of CL **1** (Supporting Information, Figure S2). DFT calculations show no charge localization on the central aromatic moiety of CL **1**. For CL **2**, a negative charge is present on this moiety and a relative lower electron density on the pyridine groups. These observations are in agreement with the  $^{15}\text{N}$  NMR data. The calculated charge distribution is hardly effected by the solvent (toluene vs.  $\text{H}_2\text{O}$ ; Supporting Information, Table S1). Apparently, the different electronic nature of the CLs is expressed in the level of AuNP aggregation and

[\*] M. Orbach, Dr. M. Lahav, Prof. M. E. van der Boom  
Department of Organic Chemistry, Weizmann Institute of Science  
Rehovot—76100 (Israel)  
E-mail: milko.vanderboom@weizmann.ac.il  
Homepage: <http://www.weizmann.ac.il/oc/vanderboom/>  
Dr. P. Milko, Dr. S. G. Wolf  
Department of Chemical Research Support  
Weizmann Institute of Science  
Rehovot—76100 (Israel)

[\*\*] This research was supported by the Helen and Martin Kimmel Center for Molecular Design and the Minerva Foundation. The transmission electron microscopy studies in aqueous solution were conducted at the Irving and Cherna Moskowitz Center for Nano and Bio-Nano Imaging at the Weizmann Institute of Science. M.E.v.d.B. is the incumbent of the Bruce A. Pearlman Professorial Chair in Synthetic Organic Chemistry.

Supporting information for this article is available on the WWW under <http://dx.doi.org/10.1002/anie.201203291>.

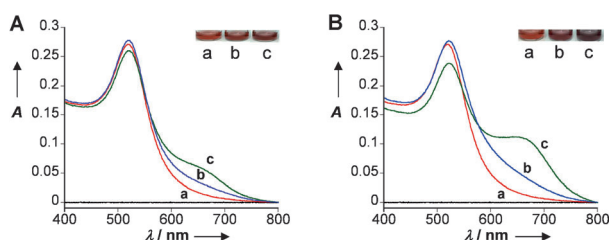


**Figure 2.** A, B) UV/Vis spectra in water of a) citrate-capped AuNPs and of the hybrid AuNP assemblies generated from mixing the AuNPs with THF solutions of b) monopyridine ligand **3** (Supporting Information, Scheme S1) or c) CL **1** at two different final concentrations of the compounds: A) 1.0 μM, B) 1.9 μM. Insets: photographs of solutions (a), (b), and (c). The spectra were recorded 2 min after mixing the components and fivefold dilution.

their optical properties. Control experiments with ligands having only one vinylpyridine group do not result in aggregation of the AuNPs (Figure 2; Supporting Information, Scheme S1).

Transmission electron microscope (TEM) images were taken to gain a qualitative representation of the hybrid AuNP assemblies in solution. The aggregates seen in those images (Figure 3 A, B) are in good agreement with the UV/Vis results (Figure 1). The reaction of CL **1** ([CL] = 1.0 μM) and citrate-capped AuNPs resulted in the formation of relatively dense assemblies (Figure 3 A). The exchange of the citrate capping layer by the CLs and the coordination of pyridine moieties to the AuNPs are confirmed by the interparticle spacing of ( $1.5 \pm 0.3$ ) nm. This observation is in good agreement with the calculated length of the CLs (1.6 nm). To rule out drying effects, we performed cryogenic (cryo-) TEM measurements

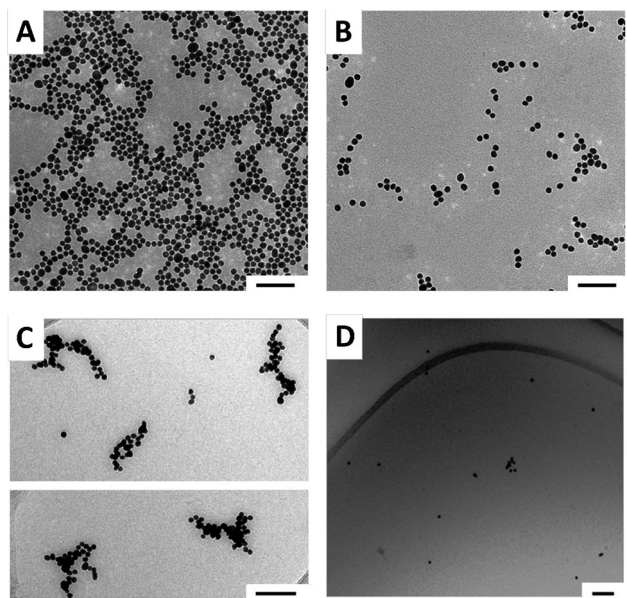


**Figure 3.** Representative TEM (top) and cryo-TEM (bottom) images of hybrid AuNP assemblies generated from mixing citrate-capped AuNPs in water with THF solutions of CL **1** (A, C) or CL **2** (B, D). Final [CL] = 1.0 μM. Scale bar = 100 nm. For additional images, see the Supporting Information, Figure S3.

with these water-soluble citrate-capped AuNPs (Figure 3 C, D). Indeed, the cryo-TEM images revealed the presence of smaller aggregates compared with the dry-TEM measured. However, the aggregation of the citrate-capped AuNPs is again more distinct with CL **1**.

These observations seem straightforward; however, aggregation of hybrid NPs is a complex phenomenon.<sup>[14,15]</sup> Interestingly, the level of aggregation with the two CLs is reversed when TOAB-capped AuNPs in toluene are used (Figure 4). For this capping-layer-solvent combination, the AuNP-aggregation is more pronounced with CL **2**. The

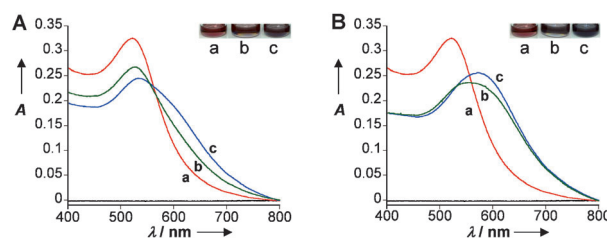


**Figure 4.** A, B) UV/Vis spectra in THF of a) TOAB-capped AuNPs and of the hybrid AuNP assemblies generated from mixing the AuNPs with THF solutions of b) CL **1** or c) CL **2** at two different final concentrations of the CL: A) 1.0 μM, B) 2.8 μM. Insets: photographs of solutions (a), (b), and (c). The spectra were recorded 2 min after mixing the components and fivefold dilution.<sup>[23]</sup>

optical behavior during the AuNP aggregation is different when the CL concentration is increased from 0.0 to 3.7 μM. Initially, a decrease in the plasmon band at  $\lambda_{\max} \approx 520$  nm is observable, which is followed by a red-shift toward  $\lambda_{\max} \approx 570$  nm. Increasing the CL concentration resulted in an increase of the absorption intensity of this band (Supporting Information, Figure S1). Control experiments show that using a monopyridine ligand does not form aggregates with TOAB-capped AuNPs (Figure 5; Supporting Information, Scheme S1). TEM images also support this trend (Supporting Information, Figure S4). Dampening of the main plasmon band was observed, showing that the stabilizing capping layer of the AuNPs was exchanged with the monopyridine ligand.<sup>[22,24]</sup> Note that the here used TOAB-AuNPs are smaller (ca. 5 nm) than citrate-AuNPs (ca. 13 nm), and thus more sensitive to damping.<sup>[25]</sup>

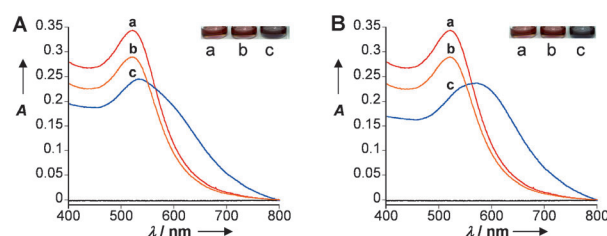


**Figure 5.** A, B) UV/Vis spectra in THF of a) TOAB-capped AuNPs and of the hybrid AuNP assemblies generated from mixing the AuNPs with THF solutions of b) ligand **4** or c) CL **2** at two different final concentrations of the compounds: A) 1.0 μM, B) 1.9 μM. Insets: photographs of solutions (a), (b), and (c). The spectra were recorded 2 min after mixing the components and fivefold dilution.

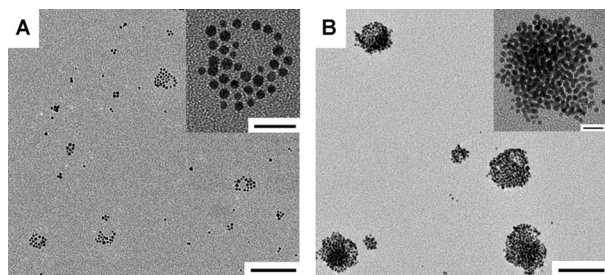


**Figure 6.** Representative TEM images of the hybrid AuNP assemblies, generated from mixing TOAB-capped AuNPs in toluene with THF solutions of A) CL 1 or B) CL 2. Final [CL] = 1.0  $\mu\text{M}$ . Scale bar = 100 nm; in the insets = 20 nm. For additional images, see the Supporting Information, Figure S7.

TEM images of hybrid AuNP assemblies generated from treating TOAB-AuNPs with CL 1 and CL 2 confirm our observations in solution (Figure 6). The AuNPs do not change their size or shape upon reacting with the CLs (Supporting Information, Figure S5). The exchange of TOAB layer by the CLs and the coordination of pyridine to the AuNPs is evident from the interparticle spacing of  $(1.5 \pm 0.3)$  nm. Cryo-TEM measurements were performed in toluene (Figure 7). As expected, smaller aggregates can be seen by cryo-TEM in comparison with the dry-TEM images using the same reaction conditions (Supporting Information, Figure S6). Nevertheless, CL 2 generates larger aggregates with TOAB-AuNP than with CL 1, which is consistent with the UV/Vis and TEM data (Figures 4 and 6).

The organic and water-soluble AuNP assemblies clearly differ in their shape and size (Figure 3 and Figure 6). The use of TOAB-capped AuNPs in toluene resulted in spherical aggregates, whereas the use of citrate-capped AuNPs in water afforded unordered and larger assemblies. Performing the reactions with TOAB-capped AuNPs in toluene or toluene/THF (1:6 v/v ratio) did not significantly influence the level and structure of the aggregates, suggesting that the solvent polarity do not play a major role in the formation of these assemblies (Supporting Information, Figures S10 and S11). Alkorta et al. showed that attractive anion- $\pi$  interactions between bromide ions and fluorinated arenes are possible.<sup>[26]</sup> Such interactions might facilitate here the penetration of CL 2

towards the TOAB-gold surface and increase the ability to aggregate the particles.<sup>[26,27]</sup> Furthermore, the hydrophobic properties of CL 2 might enhance segregation and enhance the interaction with the hydrophobic TOAB-AuNPs.<sup>[28–30]</sup> DFT calculations show that CL 1 and CL 2 have the same “flat” geometry without deviation from a horizontal plane of symmetry. Relaxed potential-energy-surface scans that correspond to rotation around carbon-carbon single bonds ( $\phi_1$  and  $\phi_2$ ) were performed (Supporting Information, Figure S12). Additionally, constrained potential-energy-surface scans were carried out with coupled rotation of two dihedral angles. The results show that the planar structures of CLs are the global minima of the potential energy surfaces (Supporting Information, Figures S13–S15). These calculations indicate that the different assembly behavior of CL 1 and CL 2 are not caused by their geometry.

In conclusion, the highest level of aggregation was observed for citrate-capped AuNPs with CL 1 in water and for TOAB-capped AuNPs with CL 2 in toluene. The large differences between the formation of AuNP assemblies with CLs 1 and 2 both in water and in toluene using citrate- and TOAB-capped AuNPs, respectively, while keeping other parameters constant, clearly demonstrates that electronic factors and/or hydrophobic interactions are involved. The differences observed between CL 1 and 2 is unlikely to be a result of their geometry but might reflect their different electronic structure. DFT calculations show that coordination of one of the pyridine units to the gold surface of Au<sub>8</sub> does not influence the charge on the second pyridine. Therefore, the electronic factors governing the AuNP assembly are likely to be similar for the initial coordination of the CLs to the individual NPs and the subsequent cross-linking (Supporting Information, Tables S2–S4). However, we cannot exclude that the different sizes of the citrate- and TOAB-capped AuNPs does not affect their aggregation. Previous studies have highlighted the importance of the molecular geometry of CLs, but not their electronic properties.<sup>[14,15,31]</sup> Furthermore, the significant differences between the water and toluene systems show that the capping layer-solvent combination are also pivotal parameters that affect the aggregation of AuNPs. Although the precise role of each individual reaction parameter (namely capping layer, solvent, CL) is not fully understood, they can be applied to control the level of AuNP aggregation.<sup>[25,32–36]</sup>

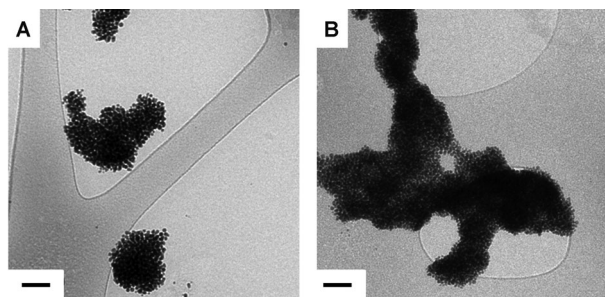


**Figure 7.** Representative cryo-TEM images of the hybrid AuNP assemblies generated from mixing TOAB-capped AuNPs in toluene with THF solutions of A) CL 1 or B) CL 2. Final [CL] = 3.7  $\mu\text{M}$ . Scale bar = 50 nm. For additional images, see the Supporting Information, Figures S8, S9.

Received: April 29, 2012

Published online: June 13, 2012

**Keywords:** aggregation · cross-linking · gold · nanostructures

- [1] B. Kong, A. Zhu, Y. Luo, Y. Tian, Y. Yu, G. Shi, *Angew. Chem.* **2011**, 123, 1877–1880; *Angew. Chem. Int. Ed.* **2011**, 50, 1837–1840.
- [2] D. Baranov, L. Manna, A. G. Kanaras, *J. Mater. Chem.* **2011**, 21, 16694–16703.
- [3] M. R. Jones, K. D. Osberg, R. J. MacFarlane, M. R. Langille, C. A. Mirkin, *Chem. Rev.* **2011**, 111, 3736–3827.



- [4] R. de laRica, R. M. Fratila, A. Szarpak, J. Huskens, A. H. Velders, *Angew. Chem.* **2011**, *123*, 5822–5825; *Angew. Chem. Int. Ed.* **2011**, *50*, 5704–5707.
- [5] T. Shirman, T. Arad, M. E. van der Boom, *Angew. Chem.* **2010**, *122*, 938–941; *Angew. Chem. Int. Ed.* **2010**, *49*, 926–929.
- [6] D. A. Giljohann, D. S. Seferos, W. L. Daniel, M. D. Massich, P. C. Patel, C. A. Mirkin, *Angew. Chem.* **2010**, *122*, 3352–3366; *Angew. Chem. Int. Ed.* **2010**, *49*, 3280–3294.
- [7] A. N. Shipway, E. Katz, I. Willner, *ChemPhysChem* **2000**, *1*, 18–52.
- [8] J.-M. Nam, C. S. Thaxton, C. A. Mirkin, *Science* **2003**, *301*, 1884–1886.
- [9] X. Xu, W. L. Daniel, W. Wei, C. A. Mirkin, *Small* **2010**, *6*, 623–626.
- [10] Y. Zhou, S. Wang, K. Zhang, X. Jiang, *Angew. Chem.* **2008**, *120*, 7564–7566; *Angew. Chem. Int. Ed.* **2008**, *47*, 7454–7456.
- [11] M. Grzelczak, J. Vermant, E. M. Furst, L. M. Liz-Marzan, *ACS Nano* **2010**, *4*, 3591–3605.
- [12] R. Klajn, M. A. Olson, P. J. Wesson, L. Fang, A. Coskun, A. Trabolsi, S. Soh, J. F. Stoddart, B. A. Grzybowski, *Nat. Chem.* **2009**, *1*, 733–738.
- [13] R. Klajn, K. J. M. Bishop, B. A. Grzybowski, *Proc. Natl. Acad. Sci. USA* **2007**, *104*, 10305–10309.
- [14] L. Beverina, *ChemPhysChem* **2010**, *11*, 2075–2077.
- [15] R. Kaminker, M. Lahav, L. Motiei, M. Vartanian, R. Popovitz-Biro, M. A. Iron, M. E. van der Boom, *Angew. Chem.* **2010**, *122*, 1240–1243; *Angew. Chem. Int. Ed.* **2010**, *49*, 1218–1221.
- [16] M. Altman, M. Rachamim, T. Ichiki, M. A. Iron, G. Evmenenko, P. Dutta, M. E. van der Boom, *Chem. Eur. J.* **2010**, *16*, 6744–6747.
- [17] M. Altman, A. D. Shukla, T. Zubkov, G. Evmenenko, P. Dutta, M. E. van der Boom, *J. Am. Chem. Soc.* **2006**, *128*, 7374–7382.
- [18] H. Detert, U. Stalmach, E. Sugiono, *Synth. Met.* **2004**, *147*, 227–231.
- [19] The TOAB-AuNP stock solution was diluted with toluene to give the same absorption intensity as that of the citrate-capped AuNPs.
- [20] A. E. Saunders, M. B. Sigman Jr., B. A. Korgel, *J. Phys. Chem. B* **2004**, *108*, 193–199.
- [21] O. Balmes, J. O. Malm, G. Karlsson, J. O. Bovin, *J. Nanopart. Res.* **2004**, *6*, 569–576.
- [22] G. K. Thomas, J. Zajicek, P. V. Kamat, *Langmuir* **2002**, *18*, 3722–3727.
- [23] Hybrid AuNP assemblies generated from mixing citrate-capped or TOAB-capped AuNPs with THF solutions of CL **1** or CL **2** show about 8% scattering: A. B. Tesler, L. Chuntanov, T. Karakouz, T. A. Bendikov, G. Haran, A. Vaskevich, I. Rubinstein, *J. Phys. Chem. C* **2011**, *115*, 24642–25652.
- [24] Y.-S. Shon, C. Shaeleen, P. Voundi, *Colloids Surf. A* **2009**, *352*, 12–17.
- [25] M.-C. Daniel, D. Astruc, *Chem. Rev.* **2004**, *104*, 293–346.
- [26] I. Alkorta, I. Rozas, J. Elguero, *J. Am. Chem. Soc.* **2002**, *124*, 8593–8598.
- [27] M. Giese, M. Albrecht, C. Bannwarth, G. Raabe, A. Valkonen, K. Rissanen, *Chem. Commun.* **2011**, *47*, 8542–8544.
- [28] L. Patrone, V. Gadenne, S. Desbief, *Langmuir* **2010**, *26*, 17111–17118.
- [29] M. P. Krafft, J. G. Riess, *Biochimie* **1998**, *80*, 489–514.
- [30] M. Hird, *Chem. Soc. Rev.* **2007**, *36*, 2070–2095.
- [31] H. Yan, S. I. Lim, L.-C. Zhang, S.-C. Gao, D. Mott, Y. Le, R. Loukrakpam, D.-L. An, C.-J. Zhong, *J. Mater. Chem.* **2011**, *21*, 1890–1901.
- [32] *Nanoparticle Assemblies and Superstructures* (Ed.: N. A. Kotov), Taylor & Francis, Boca Raton, FL, **2006**.
- [33] *Metal Nanoparticles: Synthesis Characterization, and Applications* (Eds.: D. L. Feldheim, C. A. Foss, Jr.), Marcel Dekker, New York, **2002**.
- [34] *Nanoparticles: From Theory to Application* (Ed.: G. Schmid), Wiley-VCH, Weinheim, **2004**.
- [35] B. L. V. Prasad, C. M. Sorensen, K. J. Klabunde, *Chem. Soc. Rev.* **2008**, *37*, 1871–1883.
- [36] S. K. Ghosh, T. Pal, *Chem. Rev.* **2007**, *107*, 4797–4862.